Inorganic Chemistry

Article

pubs.acs.org/IC

Selectivity of Azine Ligands Toward Lanthanide(III)/Actinide(III) Differentiation: A Relativistic DFT Based Rationalization

Abdellah Zaiter,[†] Boudersa Amine,[†] Yamina Bouzidi,[†] Lotfi Belkhiri,*[,†] Abdou Boucekkine,*[,‡] and Michel Ephritikhine[§]

[†]URCHEMS, Université Constantine 1 (ex. Mentouri), route de Ain El Bey, 25017 Constantine, Algeria

[‡]Institut des Sciences Chimiques de Rennes, UMR 6226 CNRS-Université de Rennes 1, Campus de Beaulieu, 35042 Rennes Cedex, France

[§]CEA, IRAMIS, NIMBE, CNRS UMR 3299, CEA/Saclay, 91191 Gif-sur-Yvette, France

Supporting Information

ABSTRACT: Polyazines emerge as highly selective ligands toward actinide versus lanthanide separation. Electronic structures of several mono- and polyazine f-complexes of general formula MX3L (M^{+3} = Ce, Nd, Eu, U, Am, and Cm; X = RCp^- or NO_3^-; L = N-donor ligand) related to Ln^{III}/An^{III} differentiation have been investigated using scalar relativistic ZORA/DFT calculations. In all cases, DFT calculations predict shorter An−N bonds than Ln−N ones whatever the azine used, in good agreement with available experimental data. The An−N bonds are also characterized by higher stretching frequencies than Ln−N bonds. The electronic structures of all species have been studied using different population analyses, among them natural population (NPA) and the quantum theory of atoms in molecule approach (QTAIM), as well as using different bond indices. The ability for Ln^{III}/An^{III} differentiation of the terdentate bipyrazolate BPPR ligand in the $M(BPPR)(NO_3)_3$ complexes (M^{3+} = Ce, Eu, U and Am ; R = H, 2,2-dimethylpropyl) where BPP = 2,6-bis(dialkyl-1*H*-pyrazol-3-yl)pyridine has been studied, with a special emphasis on the total metal−ligand bonding energy (TBE). The ZORA/DFT approach was found to properly reproduce the higher selectivity of the polyazine BPP ligand compared to monoazines, especially for the Eu^{III}/Am^{III} pair operating in spent nuclear fuel, using computed TBEs as criterion. Moreover, the orbital part of the total bonding energy appears also to rationalize well the observed selectivity.

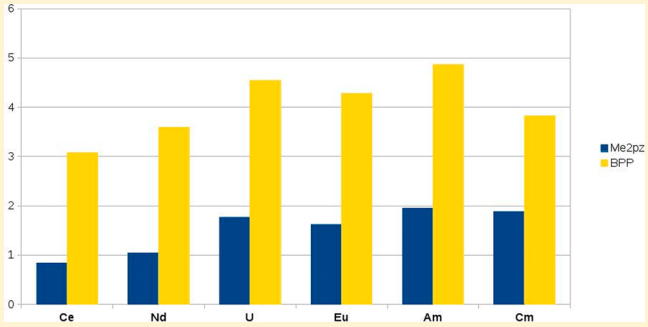

INTRODUCTION

Separation of trivalent actinides An^{III} from lanthanides Ln^{III} ions, especially radioactive minor actinides (Am, Cm) from lanthanide products of fission (Eu), is a key step in the nuclear waste partitioning strategy.[1,2] Much attention has been paid to ligands that would favor the selective complexation of actinides(III) over lanthanides(III) in liquid/liquid solvent extraction processes.[3,4] Although f ions are considered as hard acidic cations according to Pearson's HSAB theory,[5] primary actinides 5f ions are known to be slightly less hard than lanthanides 4f congeners. As a consequence, various studies have shown that a selective complexation of trivalent An^{III} over Ln^{III} ions could be reached by using soft donor ligands containing atoms such as S, N, or P elements.[3]

In fact, N-heterocyclic ligands have been the subject of numerous studies related to their interesting selectivity in extracting processes from nitric acidic solutions into an organic phase.[6−12] Of particular interest are terdentate planar ligands such as terpyridine (terpy), the BTP (2,6-bis(1,2,4-triazin-3-yl)pyridine),[12a−d] tripodal oligoamines such as tpza (tris[(2-pyrazinyl)methyl]amine),[12e] and tptz (2,4,6-tris(4-alkyl-2-pyridyl)-1,3,5-triazine) Lewis bases.[12f] These ligands give rise to Ln^{III}/An^{III} separation factors ranging from *ca.* 10 for tpza, terpy, and tptz and up to 150 for BTP.[12g] Previous computational studies,[13] carried out on $[M(terpy)_3]^{3+}$ and $[M(BTP)_3]^{3+}$ model cations (M^{3+} = Ce, La, and U), have shown much better performances of BTP relatively to terpy for the selective complexation of U^{III} over Ln^{III} in solution. As stated by the authors, in all observed terdentate polyazine species, i.e., terpy and BTP complexes, M−N(BTP) bond lengths are shorter than those of M−N(terpy), in perfect agreement with their crystal structures.[13]

In 2004, Mehdoui et al.[14] studied the competitive reactions between $M(C_5H_4R)_3$ metallocenes (M = Ce, U) and monoazine molecules with implications for the actinides(III) and lanthanides(III) partitioning. More recently, highly selective polyazine ligands for Ln^{III}/An^{III} separation have been reported by several authors,[15−17] showing that preorganization of N-donor ligands considerably improves the An^{III}

Received: February 13, 2014
Published: April 22, 2014

   dx.doi.org/10.1021/ic500361b | *Inorg. Chem.* 2014, 53, 4687−4697

extraction properties. Indeed, the current strategies for the ligand design of minor actinide-selective reagents chosen for example in a SANEX-13l process must fulfill several challenging criteria such as a good level of selectivity toward the actinides, high solubility, and high resistance toward acid hydrolysis and radiolysis, and no formation of degradation products during the reprocessing.

This can be exemplified by the recent emergence of the bis(dialkyltriazinyl) reagents such as 2,6-bis(5,6-dialkyl-1,2,4-triazin-3-yl)pyridine (BTPs),[15b] bistriazinyl-2,2′:6′,2″-terpyridine (BTTP),[15c] 6,60-bis(5,6-dialkyl-1,2,4-triazin-3-yl)-2,20-bipyridines (BTBPs),[15e,f] and their phenanthroline (BTBPh) analogues, i.e., the 2,9-bis(1,2,4-triazin-3-yl)-11,10-phenanthroline ligand,[15g] or as recently reported, the 2,6-bis(5-(2,2-dimethylpropyl)-1*H*-pyrazol-3-yl)pyridine (C5-BPP) ligand.[15d] These polyazine molecules separate minor trivalent actinides(III) (e.g., Am^{3+}, Cm^{3+}) present in the nuclear spent fuel from the lanthanides(III) (e.g., Eu^{3+}, Yb^{3+}) with remarkably high efficiency and fast extraction kinetics compared to their classical terdentate (terpy, BTP, etc.) congeners. Indeed, typically, in the tetradentate ligands cases, separation factors for Am^{III} over Eu^{III} of 100−300 are achieved.[16e,f]

Recently, bis(1,2,4-triazine) ligands have also been studied theoretically by means of quantum mechanics calculations and molecular dynamics,[16] in order to shed more light on the origins of their excellent extraction properties. In the case of the quadridentate BTBP ligand, it has been found that the changes of Gibbs free energy play an important role for Am^{III}/Eu^{III} separation.[16a] In their related experimental and DFT studies, the authors concluded that, in the more favorable complexation reaction $M(NO_3)_3(H_2O)_4 + L \rightarrow ML(NO_3)_3+4H_2O$ (M^{3+} = Am or Eu ; L = BTBPs) at the interface between water and the organic phase, the formation of $Am(BTBPs)(NO_3)_3$ is found to be more energetically favorable than Eu^{III} counterparts.[16a−c] However, the authors indicate at the DFT/RECP/B3LYP level of theory that the covalence in M−L bonds, which have mainly ionic features, play a negligible role in the coordination process.

Thus, preorganization of polyazine ligands plays a crucial role in Ln^{III}/An^{III} differentiation.[12−17] Furthermore, as was recently highlighted by several authors,[13a−c,16a−c,17] thermodynamic data are important for the polyazine selectivity toward An^{III} over Ln^{III} and might also provide interesting insights on coordination chemistry with trivalent f-elements and energetic factors that could improve Ln^{III}/An^{III} discrimination.

In regard to the great importance of metallocene complexes, we found it interesting to reinvestigate computationally by means of relativistic ZORA/DFT method, the electronic structure, and metal−azine energetic bonding analysis of $M(C_5H_4R)_3$(azine) (M^{+3} = Ce, Nd, Eu, U, Am, Cm; R = H, ^{t}Bu, $SiMe_3$) metallocene models, related to Ln^{III}/An^{III} differentiation. We shall focus our study, first on the monodentate 3,5-dimethylpyrazine (Me_2pz), which was revealed as one of the best selective monoazine ligand for Ce^{III}/U^{III} differentiation[14] and considered as a basic unit for the heterocyclic polyazine reagents.[17d] Then, the study will be extended to the more useful terdentate bipyrazole BPPR ligand with BPP = 2,6-bis(dialkyl-1*H*-pyrazol-3-yl)pyridine, and R is either a hydrogen for the unsubstituted BPPH form or 2,2-dimethylpropyl for the real (C5-BPP) complex case.[15d]

The present study aims also to get more clear-cut insights into the electronic and/or steric and energetic factors which could govern Ln^{III}/An^{III} differentiation for the complexes under consideration. It is hoped that quantum chemical criteria, permitting the rationalization of the observed differentiation, could be brought to light.

COMPUTATIONAL DETAILS

All molecular geometries of mono- and polyazine compounds of general formula MX3L (M^{+3} = Ce, Nd, Eu, U, Am, Cm ; X = RCp^-, X = NO_3^- ; L = azine, BPPR) were fully optimized at the DFT level of theory, starting from X-ray structures when available. The calculations were carried out using relativistic corrections being introduced via the zero order regular approximation (ZORA).[18,19] These ZORA/DFT calculations were performed using the Amsterdam density functional (ADF2012.01) program package.[20] The Vosko−Wilk−Nusair functional (VWN)[21a] for the local density approximation (LDA) and gradient corrections for exchange and correlation of Becke and Perdew,[21b,c] respectively, i.e., the BP86 functional, have been used, particularly for the geometry optimizations and the analytical computation of the frequencies of the normal modes of vibration. In addition, single point B3LYP[21d,e] calculations have also been carried out. Triple-ζ Slater-type valence orbitals (STO) augmented by one set of polarization functions were used for all atoms.

Several theoretical studies have shown that such a ZORA/BP86/TZP approach reproduces the experimental geometries and ground state properties of f-element compounds with a satisfying accuracy.[22,23]

For all elements, the basis sets were taken from the ADF/ZORA/TZP database. For the BP86 geometry optimizations, the frozen-core approximation, where the core density is obtained from four-component Dirac−Slater calculations, has been applied for all atoms. The 1s core electrons were frozen, respectively, for carbon C[1s] and nitrogen N[1s]. The Ln[4d] and An[5d] valence space of the heavy elements includes the 4f/5s/5p/5d/6s/6p and 5f/6s/6p/6d/7s/7p shells, respectively (small core approximation).

In order to provide a better understanding of the metal−ligand bonding, a natural population analysis (NPA)[24a−c] and a quantum theory atom-in-molecules (QTAIM)[24d] analysis have been carried out in addition to a Mulliken population analysis (MPA).[24e] Although global trends are correctly reproduced in a homologous series of molecules by MPA, NBO and QTAIM topological approaches have been shown to lead to useful descriptors of the electron density distribution[24a−e] which have been used successfully for f-element complexes.[24f,25] In fact, as stated recently by Kaltsoyannis et al.,[25a−d] relevant QTAIM data lead to good correlation with the strength of chemical bonds, such as metal−ligand bonding and other closed shell interactions, e.g., hydrogen bond systems, halogen bonding. Among QTAIM descriptors are the points of lowest electron density between each atoms pair, i.e., bond critical points (BCP) for which electron density ρ_c, its Laplacian $\nabla^2\rho_c$ and energy density H_c can be defined (the subscript indicates the electron density at the BCP). As was established by previous significant work in this area,[25a−e] bonding interactions may be characterized according to these characteristic data (ρ_c, $\nabla^2\rho_c$ and H_c). Indeed, the values of ρ_c > c. 0.2 e/bohr^3 are typical of covalent (shared shell) interactions, and those of ρ_c < c. 0.1 e/bohr^3 indicate more ionic interactions (closed shell interactions). Energy density H_c is negative for bonding interactions (covalent electrons), and $\nabla^2\rho$ is generally significantly less than zero for such interactions, in relation with the concentration of electron density along the bond path linking the bonded atoms.

dx.doi.org/10.1021/ic500361b | Inorg. Chem. 2014, 53, 4687−4697

A subsequent contribution from the same authors,[25a] and references therein, reported that the magnitude of the electron density ρ_c and other QTAIM parameters at bond critical points (BCPs) show an even better correlation with bonding energy (R^2 = 0.998). All authors[25a−e] conclude that QTAIM can be used as a tool to predict the strength of bonds that contain a significant degree of covalence, especially for f-element compounds.

Finally, for all complexes, we considered the highest (2*S* + 1) spin state as the ground state configuration, i.e., doublet (f^1) spin states for the Ce^{III} systems, quartet (f^3) for Nd^{III} and U^{III} ones, heptuplet (f^6) for Eu^{III} and Am^{III}, and octuplet (f^7) spin state for Cm^{III} cases.

As ADF program supplies an energetic decomposition of the metal−ligand bonding into chemically useful terms, we have carried out spin-unrestricted fragment calculations considering the two molecular neutral moieties in interaction, i.e., MX_3 and L both for $M(RCp)_3$(azine) and $M(NO_3)_3$(BPPR) species. We remind the reader that this energetic decomposition, which is based on the transition-state method developed by Morokuma, and then by Ziegler et al.,[26a−c] provides insights into the balance of the different bonding electronic or electrostatic factors at work between the isolated cation or metallic moiety and the ligands in a complex.

Thus, within this scheme, the resulting total bonding energy TBE_{frag} between two fragments can be decomposed into two terms as follows:

$$TBE_{frag} = E_{steric} + E_{orb}$$

Here, the E_{steric} term is, in our case, the steric interaction energy between the MX_3 metallic fragment and N-donor L ligand, and E_{orb} is the orbital (covalent) contribution to the metal−azine bond. The steric energy term (E_{steric}) is itself decomposed into a destabilizing term E_{Pauli}, the electronic repulsion due to the Pauli principle, and E_{ES}, the stabilizing electrostatic energy between the two fragments:

$$E_{steric} = E_{Pauli} + E_{ES}$$

The BP86 and B3LYP bonding energies have been computed using the all electron ADF/ZORA/TZP basis set and the ZORA/BP86 optimized geometries.

RESULTS AND DISCUSSION

We start our study considering the series of triscyclopentadienyl $M(RCp)_3(Me_2pz)$ complexes (M^{+3} = Ce, Nd, Eu, U, Am, and Cm) bearing a monoazine ligand, namely, 3,5-dimethylpyrazine Me_2pz. As aforementioned, it has been shown experimentally that this azine ligand is very selective regarding the Ce^{III}/U^{III} pair.[14]

In Table 1, we report relevant computed structural parameters, M−N and average M−C, M−Cp(centroid), and N−C distances of the optimized $M(TMSCp)_3(Me_2pz)$ structures (Figure 1) compared to available experimental data. The optimized distances are in good agreement with the X-ray ones.

A shortening of the actinide M−N and M−Cp(centroid) bond distances relative to those of the lanthanide homologue, opposite to their ionic radii, is observed in all cases. For instance, the computed M−N distances for the Nd/U pair are, respectively, equal to 2.608 and 2.549 Å, whereas for the Eu/Am pair these values are 2.614 and 2.562 Å, knowing that the ionic radii of the latter pair of ions are, respectively, equal to 0.947 for Eu and 0.980 Å for Am. This bond length decrease

Table 1. ZORA/BP86 Computed and X-ray Average Distances (Å) of the $(TMSCp)_3M(Me_2pz)$ (M^{3+} = Ce, Nd, U, Eu, Am, Cm) Complexes

M^{III}, spin state	M−N	⟨M−C⟩[a]	⟨M−Cp⟩[a,b]	⟨N−C⟩[a,c]
Ce(f^1) doublet	2.679	2.889	2.623	1.347
X-ray	2.689	2.836	2.571	1.343
Nd(f^3) quartet	2.608	2.953	2.697	1.344
U(f^3) quartet	2.549	2.795	2.532	1.369
X-ray	2.656	2.812	2.543	1.343
Eu(f^6) heptuplet	2.614	2.880	2.613	1.359
Am(f^6) heptuplet	2.562	2.842	2.572	1.362
Cm(f^7) octuplet	2.539	2.853	2.584	1.368

[a]Average values. [b]Cp centroid. [c]Computed N−C distance in free Me2pz = 1.337 Å.

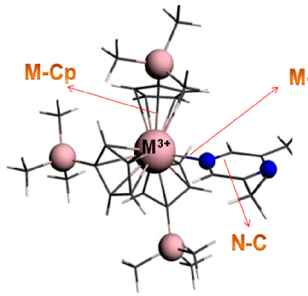

Figure 1. ZORA/BP86 optimized structure of $M(TMSCp)_3(Me_2pz)$.

when passing from a Ln^{III} to a An^{III} homologous complexes is generally understood as indicative of a more important covalent character of the actinide metal−ligand bonding. This point will be discussed later in the text.

In Table 2 are given both MPA and NPA results obtained at the ZORA/BP86 level for the $M(TMSCp)_3(Me_2pz)$ open-shell systems, Mulliken and natural metal and nitrogen atomic net charges as well as the metallic spin populations ρ(M) (second column of Table 2) which are computed as the difference between the total α and β spin electronic populations of the metal. The overlap populations of the M−N and N−C bonds are also shown. The overlap population for chemical bonds should be indicative of the degree of covalence. Very small overlap populations in M−L bonds should indicate that the ionic interaction is predominant, as stated by different authors.[16a−c]

As aforementioned (see Computational Details), MPA leads to net charges that are generally too low,[24e] thus suggesting overestimated covalent interactions in comparison to the NPA approach. The trends are the same: the natural metallic net charges (q_M), which are higher than the MPA ones, indicate also that electron density is transferred from the azine ligand to the metal, so that the metal charge decreases (q_M < 3) as the metal cation retrieves electrons. This trend is particularly pronounced for U^{III} species whose natural metallic charge (2.08) is significantly smaller than the other elements.

As usually found, the highest M−N overlap populations in the U^{III} complex are symptomatic of the more pronounced covalent character whereas its lowest N−C population is indicative of a significant metal-to-ligand π back-donation. The latter effect agrees well with U^{III} lower spin density (2.58, NPA) than the ion formal value of 3, and with the computed higher nitrogen net charge (−0.56).

dx.doi.org/10.1021/ic500361b | Inorg. Chem. 2014, 53, 4687−4697

Table 2. ZORA/BP86 MPA and NPA Results

M^{III}, spin state MPA/NPA	spin population ρ(M)	net charges		overlap populations	
		q_M	N	M−N	⟨N−C⟩
Ce(f^1) doublet	0.79/0.81	+1.81/+2.38	−0.46/−0.52	0.060/0.129	0.440/1.062
Nd(f^3) quartet	3.31/3.22	+1.41/+2.23	−0.46/−0.51	0.068/0.089	0.441/1.059
U(f^3) quartet	2.62/2.58	+0.83/+2.08	−0.51/−0.56	0.148/0.330	0.378/1.024
Eu(f^6) heptuplet	6.68/6.51	+1.34/+2.28	−0.44/−0.47	0.086/0.084	0.450/1.068
Am(f^6) heptuplet	6.44/6.23	+0.82/+2.11	−0.46/−0.50	0.119/0.141	0.426/1.049
Cm(f^7) octuplet	6.97/6.85	+0.92/+2.35	−0.46/−0.48	0.102/0.125	0.434/1.087

It is worth noting that NPA M−N overlap populations for actinide species are significantly higher than those obtained for their lanthanide counterparts, except cerium which exhibits a relatively high value. In particular, comparing the Eu and Am species the higher value of the natural M−N overlap population for the latter metal can be seen, i.e., 0.084 versus 0.141.

Bond Order Analysis. Bond multiplicities analyses are of importance when investigating bonding patterns of transition-metal complexes. Mayer bond order approach[26d] has been successfully used as a useful tool in this context.[25d,26e] More recently, another alternative is offered by Nalewajski−Mrozek (NM) bond multiplicities.[26f−i] Unlike the Mayer definition of bond orders, the Nalewajski−Mrozek valence indices comprise both covalent and ionic contributions and appear to describe more accurately experimental structural properties.[26h,i] It is noteworthy that the Nalewajski−Mrozek method gives higher M−N bond-orders than Mayer's does.

In Table 3, we report the computed Nalewajski−Mrozek (NM) and Mayer bond indices for the M−N and N−C bonds.

Table 3. ZORA/BP86 Nalewajski−Mrozek (NM) and Mayer Bond Orders

	M−N				N−C (free)[a]		
M^{III}	ω cm^{-1}	d (Å)	NM	Mayer	d (Å)	NM (1.602)	Mayer (1.433)
Ce	95	2.679	0.457	0.217	1.357	1.490	1.320
Nd	86	2.608	0.426	0.250	1.375	1.494	1.322
U	122	2.549	0.862	0.545	1.372	1.391	1.204
Eu	98	2.614	0.224	0.204	1.370	1.510	1.343
Am	103	2.562	0.303	0.345	1.379	1.472	1.292
Cm	103	2.539	0.466	0.293	1.378	1.460	1.310

[a]Bond orders of the free Me_2pz ligand given in parentheses.

In the second column of this table are also given the frequencies ω (cm^{-1}) of the M−N stretching, computed at the same level of theory.

Here again NM and Mayer analyses indicate more important metal−nitrogen bond orders for actinide complexes compared to their lanthanides congeners, correlating well with structural features and MPA/NPA results. The stretching frequencies of the M−N bonds are rather low and do not differentiate spectacularly the Ln and An coordinations. Nevertheless, it can also be seen that these stretching frequencies as indicators of bond strengths vary in the same way as Mayer, NPA, or Nalewajski−Mrozek bond indices. The bonding energy between the metal fragment and the azine ligand will be discussed in more detail later in the text.

Furthermore, the N−C bond orders are lower compared to the free monoazine ligand, likely to indicate a more important ligand-to-metal donation as well as metal-to-ligand π back-donation effects especially in the An^{III} cases, as previously stated, reaching a minimum value for the U^{III} species.

Molecular Orbital (MO) Analysis. MO frontier diagrams of the trivalent $(TMSCp)_3M(Me_2pz)$ complexes are displayed in Figure 2 for the series (M^{+3} = Ce, Nd, U) and in Figure 3 for the series (M^{+3} = Eu, Am, and Cm). For the sake of simplicity the α spin MOs only are displayed.

In these figures, the percentages %(d/f/TMSM/Me_2pz) represent, respectively, the d and f metal orbital contributions to the frontier MOs, and the total metallic molecular $(TMSCp)_3M$ fragment as well as the Me_2pz weights.

For the (M^{+3} = Ce, Nd, U) series, the diagram shows that the highest occupied α spin-orbitals, i.e., SOMO, SOMO−1, and SOMO−2 in Nd^{III} and U^{III} f^3 complexes and the SOMO in the Ce^{III} f^1 counterpart, are essentially metallic, with a strong f orbital character as indicated by the percentage orbital composition %(d/f/TMSM/Me_2pz). In the U^{III} case, the MO #102 (SOMO−1) is indicative of an important metal-to-azine π^* back-donation, whereas this interaction is much weaker in Ln^{III} complexes as illustrated by their SOMO and SOMO−2 for Ce^{III} and Nd^{III}, respectively. Indeed, the weight of the azine in the latter SOMOs shows a quite lower contribution for the Ln^{III} complexes comparatively to the corresponding SOMO−1 (MO #102) in the U^{III} complex, i.e., 8.5−12.7% versus 25.7%. Thus, the more important contribution of the Me_2pz π^* MO in U^{III} relative to Ln^{III} complexes makes clear the strongest metal-to-ligand back-donation in the uranium case.

Concerning the second (M^{+3} = Eu, Am, and Cm) series of complexes (Figure 3), the same trend is found with the six higher SOMOs being essentially metallic, with a strong f orbital character. Furthermore, the MO comparison between the Eu^{III} and Am^{III} species reveals in the latter the presence of a π back-donation effect evidenced by the SOMO−2 (MO #104A) which supports the MPA results (Table 2) leading to a significantly higher Am−N overlap population than in the Eu counterpart (i.e., 0.119 vs 0.086) as well as the NM and Mayer bond order analyses (Table 3). Thus, it appears that a covalent factor, presumably slight, could account for Eu^{III}/Am^{III} differentiation. The difference with the Cm complex, which does not exhibit such back-donation, is likely to originate from the better energetic matching between metallic 5f and ligand orbitals as was recently stated by Kaltsoyannis et al.[27a]

Let us consider now bis(pyrazol)pyridine (BPP) complexes. As aforementioned, bis(triazinyl) based polyazines (e.g., BTP, BTBP, BTBPh, BTTP, etc.) emerge as highly selective ligands toward minor actinide versus lanthanide separation.[12−17] For our part, we considered bis(pyrazol)pyridine (C5-BPP) or 2,6-bis(5-(2,2-dimethylpropyl)-1*H*-pyrazol-3-yl)pyridine and its unsubstituted form displayed in Figure 4.

As reported by Bremer et al.,[15d] the N-donor C5-BPP molecule extracts selectively trivalent actinide cations over

dx.doi.org/10.1021/ic500361b | Inorg. Chem. 2014, 53, 4687−4697

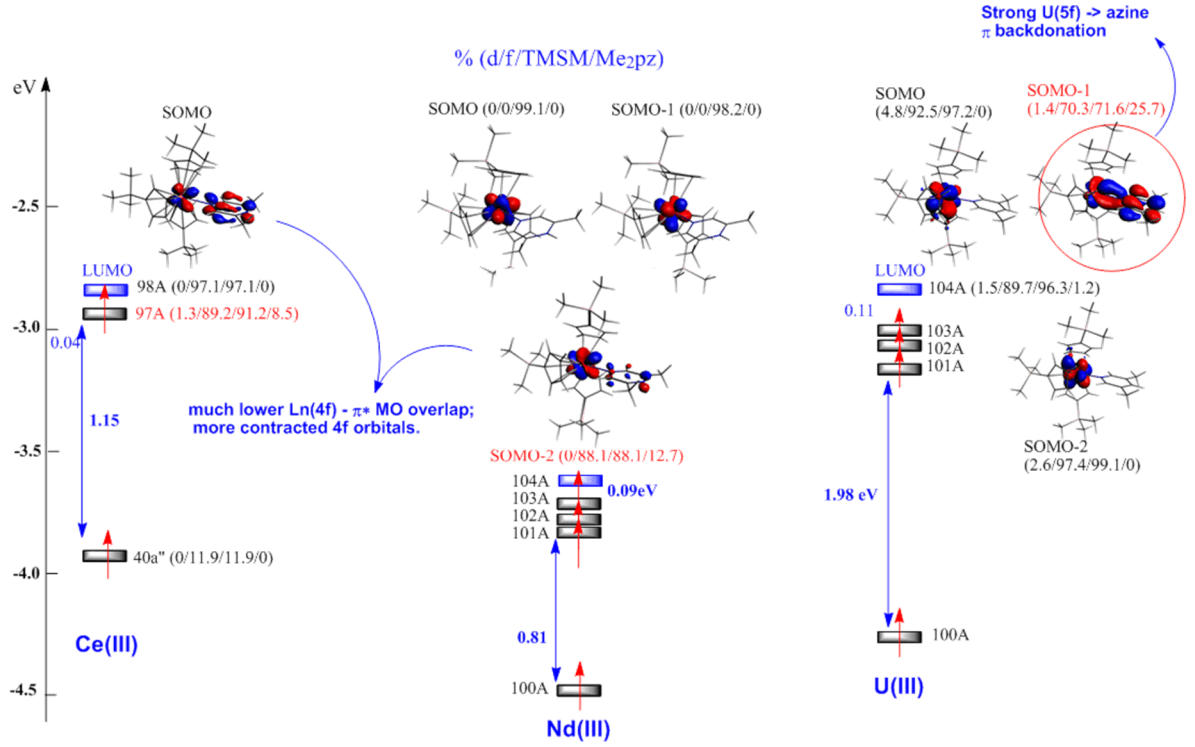

Figure 2. ZORA/BP86 α spin MO diagram for $M(TMSCp)_3(Me_2pz)$ (M^{3+} = Ce, Nd, U). Used cutoff, 0.04 e/Bohr^3.

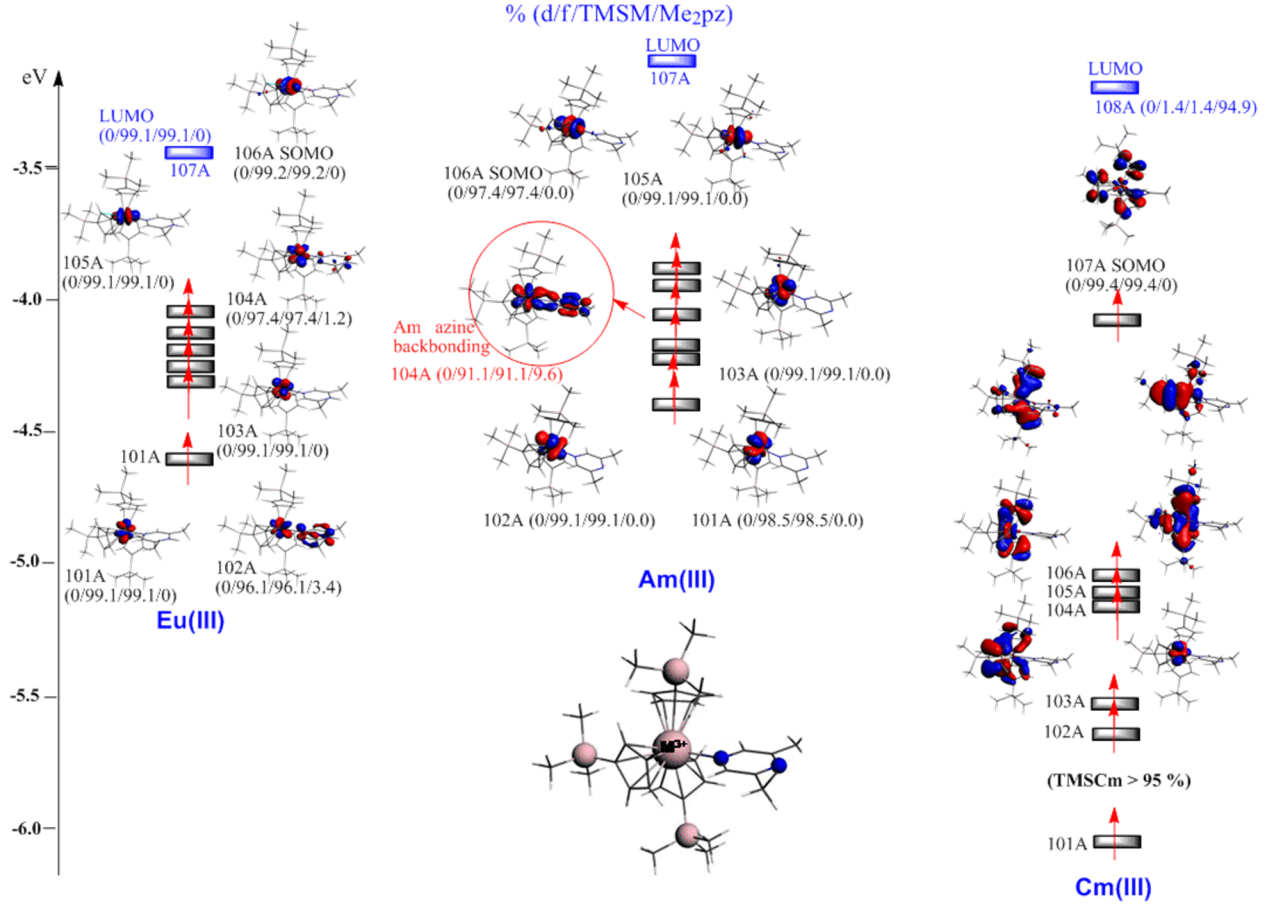

Figure 3. ZORA/BP86 α spin MO diagram for $M(TMSCp)_3(Me_2pz)$ (M^{3+} = Eu, Am, and Cm). Used cutoff, 0.04 e/Bohr^3.

dx.doi.org/10.1021/ic500361b | Inorg. Chem. 2014, 53, 4687−4697

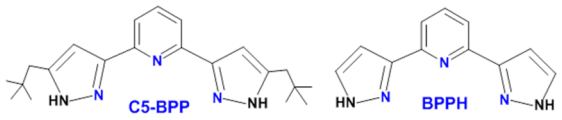

Figure 4. BPPR (R = C5, H) structures.

lanthanides, e.g., Am^{III} over Eu^{III} from up to 1 mol/L HNO_3 with a separation factor of approximately SF = 100.

In Table 4, we report the relevant optimized structural parameters of the M(C5-BPP) (M^{3+} = Ce, Nd, Eu, U, Am, Cm) complexes and of their BPPH model counterparts which are depicted in Figure 5, computed for their highest spin state as in the $M(TMSCp)_3(Me_2pz)$ case.

Table 4. ZORA/BP86 Relevant Optimized Metal−Ligand Bond Distances (Å) and Available X-ray Data[15d]

	C5BPP		BPPH	
M^{III}	$M-N_{bpz}$ (av)	$M-N_{Py}$	$M-N_{bpz}$ (av)	$M-N_{Py}$
$Ce(f^1)$	2.615−2.616 (2.615)	2.826	(2.634)	2.818
$Nd(f^3)$	2.600−2.614 (2.607)	2.805	2.611−2.622 (2.616)	2.836
$Eu(f^6)$	2.605−2.637 (2.621)	2.781	2.607−2.622 (2.614)	2.824
X-ray	2.541−2.545 (2.543)	2.622		
$U(f^3)$	2.526−2.545 (2.535)	2.639	2.528−2.544 (2.536)	2.646
$Am(f^6)$	2.576−2.581 (2.578)	2.761	2.594−2.597 (2.595)	2.813
$Cm(f^7)$	2.590−2.599 (2.594)	2.804	2.575−2.593 (2.584)	2.810

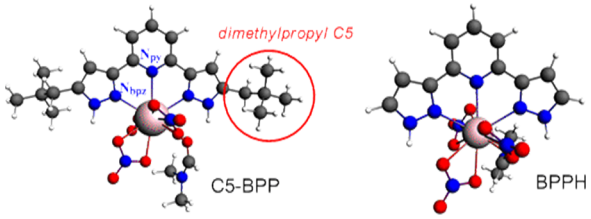

Figure 5. ZORA/BP86 optimized geometries.

In Table 4, we use the notation $M-N_{py}$ for the metal−pyridine bond distances whereas $M-N_{bpz}$ indicates the two metal−pyrazole distances (Figure 5). The metal−ligand $M-N_{bpz}$ bond distances are also given as averaged. Calculated geometries are in fair agreement with the published Eu^{III} crystal structure.[15d]

Comparison of the two computed forms, C5-BPP and BPPH, reveals that attachment of the C5 substituent leads to a reduction of the M−N distances especially at central (py) and to a lesser extent at lateral (bpz) position. These features have been already explored by previous theoretical works.[16a−c] Indeed, it was observed for M(BTBP) (1:1) Eu^{III}/Am^{III} complexes that substitution of electron-donating groups to the BTBP molecule can enhance its coordination ability and thus the energetic stability of the formed Am^{III} and Eu^{III} complexes in the gas phase.[16c] In our case, besides the fact that the U^{III} system still exhibits the shortest M−N distances, suggesting the more pronounced covalent character, the comparison between the two Eu^{III} and Am^{III} systems reveals significant differences in their metal−ligand (M−N) distances. Indeed, the $M-N_{py}$ bond distance (2.781 vs 2.761 Å) undergoes less shortening compared to $M-N_{bpz}$ (2.621 vs 2.578 Å) when passing from Eu^{III} to Am^{III}. Taking into account the difference of their ionic radii (r_{Am} = 0.980 Å; r_{Eu} = 0.947 Å),[28] the $Am-N_{bpz}$ bond is about 0.08 Å shorter than the $Eu-N_{bpz}$ bond in C5-BPP systems, on the basis of a purely ionic model. Under the same conditions, the difference between $Am-N_{py}$ and $Eu-N_{py}$ bonds is only 0.05 Å. These results may indicate higher covalence for the Am−N bonding compared to the Eu−N one (for isolated molecules). It can also be supposed from Table 4 that the BPP ligand mainly coordinates with metal ions via N_{bpz} lateral sites rather than to pyridine N_{py} central ones in minor actinides systems, because the $M-N_{bpz}$ distances are shorter than the $M-N_{py}$ ones. The electronic structure study which follows will shed light on these points.

Electronic Structures. In Table 5 are given the MPA and NPA results, i.e., atomic net charges, orbital (d/f) population, metal spin population, as well as the overlap populations of the $M-N_{bpz}$ and $M-N_{py}$ of the complexes under consideration.

Considering the BPP complexes, the same trends as for the monoazine systems (Table 2) are observed. Indeed, in the same way as MPA, it can be seen that, in all cases, NPA leads to M−N bonds exhibiting more important overlap populations for the An^{III} than for the Ln^{III} complexes. However, the metal−nitrogen overlap populations are smaller than in the case of the $M(TMSCp)_3(Me_2pz)$ species studied previously, due to the higher number of nitrogen atoms linked to the metal.

Table 5. ZORA/BP86 MPA and NPA Results for $M(C5\text{-}BPP)(NO_3)_3$ (M^{3+} = Ce, Nd, U, Eu, Am, and Cm) Complexes

		net charges				overlap population	
M^{III} spin multiplicity	metal spin population ρ_M	M^q	N_{py}	$\langle N_{bpz}\rangle$	orbital population d/f	$M-N_{py}$	$M-N_{bpz}$[a]
$Ce(f^1)$ doublet MPA	0.93	1.70	−0.41	−0.33	0.99/1.24	0.016	0.032−0.035
NPA	0.90	2.40	−0.47	−0.36	0.28/1.11	0.133	0.176−0.180
$Nd(f^3)$ quartet MPA	3.11	1.67	−0.39	−0.33	0.93/3.33	0.005	0.019−0.024
NPA	3.07	2.33	−0.44	−0.35	0.24/3.23	0.097	0.136−0.141
$U(f^3)$ quartet MPA	2.53	1.73	−0.47	−0.34	0.91/3.08	0.094	0.072−0.081
NPA	2.47	2.13	−0.48	−0.34	0.29/3.10	0.291	0.320−0.328
$Eu(f^6)$ heptuplet MPA	6.32	1.57	−0.39	−0.34	0.78/6.49	0.009	0.010−0.013
NPA	6.35	2.20	−0.44	−0.34	0.21/6.40	0.083	0.118−0.121
$Am(f^6)$ heptuplet MPA	6.13	1.55	−0.40	−0.31	0.90/6.26	0.021	0.036−0.042
NPA	6.02	2.27	−0.45	−0.34	0.22/6.30	0.132	0.168−0.170
$Cm(f^7)$ octuplet MPA	6.94	1.61	−0.39	−0.31	0.92/7.25	0.010	0.029−0.040
NPA	6.85	2.40	−0.45	−0.35	0.23/7.14	0.117	0.158−0.165

[a]Average values.

dx.doi.org/10.1021/ic500361b | Inorg. Chem. 2014, 53, 4687−4697

The Am^{III} complex is also characterized by a greater M−N(BPP) overlap population than its Eu congener, 0.036−0.042 vs 0.010−0.013, and 0.021 vs 0.009, respectively, for bipyrazolate (bpz) and pyridine (py) M−N bonding. Interestingly the M−N covalent bonding is stronger with the bpz nitrogen atoms than with the py nitrogen, which agrees well with Eu^{III}/Am^{III} structural features (Table 4). MO analysis (see Supporting Information SI-2) reveals that, contrary to the U^{III} complex, no back-donation is observed for Cm^{III} and Eu^{III} complexes, and only a slight one for Am^{III}. Thus, ligand-to-metal donation is mainly responsible for the obtained M−N overlap populations.

The NM and Mayer analyses (Table 6) confirm this trend leading to lower metal−nitrogen bond orders than those obtained for $M(TMSCp)_3(Me_2pz)$. Otherwise, in the minor actinide cases, the bond order analysis confirms the stronger $M-N_{bpz}$ coordination than $M-N_{py}$ ones, as previously highlighted by MPA and NPA analysis (Table 5). Moreover, the Am−N bonding appears to be stronger than its Eu−N congener, in agreement with the greater thermodynamic stability of the former.

Table 6. ZORA/BP86 Nalewajski−Mrozek (NM) and Mayer Bond Orders Analysis for $M(C5\text{-}BPP)(NO_3)_3$ (M^{3+}= Ce, Nd, U, Eu, Am, and Cm) Complexes

	$M-N_{py}$		$M-N_{bpz}$	
M^{III} bond order	Mayer	NM	Mayer	NM
Ce	0.185	0.367	0.236	0.470
Nd	0.133	0.213	0.185	0.273
U	0.430	0.655	0.362	0.630
Eu	0.128	0.131	0.158	0.170
Am	0.191	0.194	0.234	0.227
Cm	0.150	0.284	0.215	0.398

The computed MO diagram for the $M(C5\text{-}BPP)(NO_3)_3$ (M = Ce^{3+}, Nd^{3+}, and U^{3+}) complexes, at the ZORA/BP86 level (see Supporting Information SI-1), reveals a SOMO−2 which is stabilized by significant $U^{III}-N_{py}$ back-donation effects corresponding to U(5f) → π^* MO(BPP). This SOMO−2, with its percentage composition % (d/f/M/BPP), is depicted in Figure 6.

To further assess the extent of covalence in f-complexes, we applied to the current target systems the quantum theory of atoms-in-molecules (QTAIM).[24d,25] As aforementioned (see Computational Details), this topological method developed by Bader[24d] allows researchers to probe the covalence in an f-element−ligand bond in good agreement with experienced trends,[25] especially in the case of lanthanides(III)/actinides(III) differentiation.[25b,d,e]

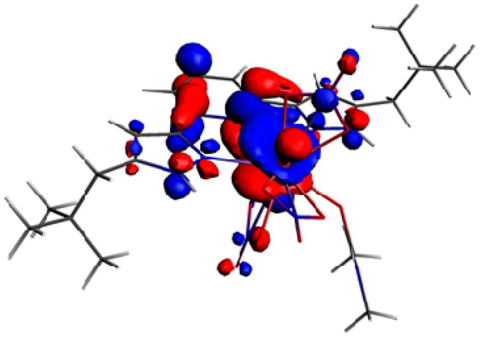

Figure 6. ZORA/BP86 $U(C5\text{-}BPP)(NO_3)_3$ SOMO−2; (d/f/M/C5-BPP) percentage composition (0/63.5/63.5/36.2). Used cutoff, 0.04 e/$Bohr^3$.

In Table 7 we report electron (ρ_c) and energy densities (H_c) data at the metal−nitrogen bond critical points for $M(C5\text{-}BPP)(NO_3)_3$ complexes.

BP86/QTAIM data show that metal−nitrogen electron densities ρ_c are low, ranging from 0.013 to 0.027 for central $M-N_{py}$ bonds and from 0.018 to 0.041 e/$Bohr^3$ for lateral $M-N_{bpz}$ coordination. Although the electron ρ_c density values increase using B3LYP calculations, as noted by previous works on f-complexes,[25] they suggest low metal−ligand covalence. This is confirmed by the energy density H_c data which are negative and small, ranging from −0.011 to −0.032 au and from −0.019 to −0.043 au at the BP86 and B3LYP levels of calculations, respectively. These AIM results, which are consistent with previous works,[25a,d] are indicative of dominant ionic metal−ligand bonding; however, it is worth noting, in the case of the Eu/Am pair, the significantly greater values obtained for the actinide complex compared to its lanthanide analogue. This is in line with the NPA analysis.

Metal−Ligand Bonding Energy Analysis. As indicated by the electronic structure analyses, the variations of structural parameters of the considered complexes could be explained by the donation and back-donation abilities of the RCp, azine, and polyazine BPP ligands and the occurrence of a higher covalent character of the bonding. However, even though structural parameters and electronic factors can account for the latter effects,[27b] they cannot usually permit us to differentiate actinide(III) and lanthanide(III) systems in terms of their relative stabilities.

In this regard, we investigated the series of MX_3L (L = azine and polyazine BPP) complexes, across the same series, considering the bonding energies between the two MX_3 and L as neutral fragments. We report in Tables 7 and 8 for $M(TMSCp)_3(Me_2pz)$ and $M(NO_3)_3(BPPR)$ complexes, respectively, the energetic decomposition analysis of the total bonding energy (TBE_{frag}) as the sum of steric E_{st} and orbital E_{orb} terms (see Computational Details), according to the formal complexation reaction scheme:

$$MX_3 + L \rightarrow MX_3L$$

The two MX_3 and L fragments keep the geometries they have in the whole complex and are not geometrically reoptimized. First, it is worth remembering that the orbital E_{orb} part includes both a polarization term due to the reorganization of the metal and ligand electronic densities with complexation and some possible covalence if their orbitals overlap.[13a] Unfortunately, these two terms cannot be evaluated separately. Moreover, it is worth noting that the basis set superposition error (BSSE) that we estimated using the counterpoise recipe was found in the range 0.05−0.09 eV, rather small in comparison to the computed TBE_{frag} values. Finally, it must be pointed out that the computations have been carried out at the unrestricted level of theory. We computed also the zero point vibration energy (ZPVE) for all complexes at the ZORA/BP86 level (given in Supporting Information SI-3) and found no difference between the values of the Ln and An species.

M−Me_2pz Energy Bonding. In the case of the $M(TMSCp)_3(Me_2pz)$ complexes, as aforementioned, the Ce^{III} complex has been found to be experimentally less stable than its U^{III} counterpart.[14] According to the enthalpy of $(RCp)_3ML$

dx.doi.org/10.1021/ic500361b | Inorg. Chem. 2014, 53, 4687−4697

Table 7. ZORA/BP86 and B3LYP QTAIM Analysis of Electron ρ_c (e/Bohr^3) and Energy Densities H_c (au) at Metal−Nitrogen Bond Critical Point for M(C5-BPP)$(NO_3)_3$ (M^{3+}= Ce, Nd, U, Eu, Am, and Cm) Complexes

ρ_c/H_c	Ce(f^1)	Nd(f^3)	U(f^3)	Eu(f^6)	Am(f^6)	Cm(f^7)
M−N_{py} BP86	0.027/−0.020	0.019/−0.021	0.026/−0.016	0.013/−0.011	0.017/−0.014	0.015/−0.013
M−N_{py} B3LYP	0.026/−0.021	nc	0.037/−0.030	0.023/−0.019	0.031/−0.026	0.028/−0.024
M−N_{bpz}[a] BP86	0.041/−0.032	0.027/−0.032	0.039/−0.023	0.018/−0.016	0.024/−0.023	0.023/−0.021
M−N_{bpz}[a] B3LYP	0.040/−0.033	nc	0.050/−0.043	0.036/−0.031	0.045/−0.040	0.043/−0.038

[a]Average values; nc, SCF did not converge.

Table 8. ZORA/BP86-B3LYP Fragment Bonding Energies (eV) and BP86/BSSE Results of $(TMSCp)_3M(Me_2pz)$ (M^{3+} = Ce, Nd, Eu, U, Am, and Cm) Complexes

M^{III} BP86/B3LYP	M−N (Å)[a]	E_{ST}	E_{orb}	TBE_{Frag}	BP86-BSSE eV (kcal/mol)
Ce	2.679	0.097/0.084	−0.847/−0.924	−0.750/−0.840	−0.045 (−1.05)
Nd	2.608	−0.001/−0.002	−0.549/−1.040	−0.550/−1.042	−0.048 (−1.13)
U	2.549	0.458/0.537	−1.744/−2.305	−1.287/−1.768	−0.061 (−1.42)
Eu	2.614	−0.012/−0.096	−1.003/−1.525	−1.015/−1.621	0.049 (−1.15)
Am	2.562	0.276/0.253	−1.342/−2.202	−1.066/−1.949	−0.052 (−1.25)
Cm	2.539	0.065/0.043	−1.239/−1.926	−1.174/−1.883	0.056 (−1.08)

[a]Metal−nitrogen distance.

Table 9. ZORA/BP86-B3LYP Fragment Bonding Energies (eV) of $M(NO_3)_3$(C5-BPP) (M^{3+} = Ce, Nd, U, Eu, Am, Cm) Complexes

M^{III} BP86/B3LYP	E_{ST}	E_{orb}	TBE_{Frag}	BP86-BSSE eV (kcal/mol)
Ce	−0.102/−0.437	−3.080/−2.642	−3.182/−3.079	−0.090 (−2.07)
Nd	−0.361/−0.755	−3.111/−2.839	−3.472/−3.594	−0.091 (−2.09)
U	0.360/0.350	−4.805/−4.894	−4.445/−4.544	−0.098 (−2.28)
Eu	−0.771/−0.797	−2.869/−3.482	−3.640/−4.279	−0.087 (−2.01)
Am	−0.321/−0.587	−3.377/−4.273	−3.698/−4.860	−0.109 (−2.51)
Cm	−0.041/−0.260	−3.211/−3.565	−3.253/−3.825	−0.095 (−2.21)

formation, the same conclusions were drawn for the observed greater exothermicity of the U^{III} complexes than their Ce^{III} counterparts.

As shown in Table 8, for $M(TMSCp)_3(Me_2pz)$ (Ce^{3+}, Nd^{3+}, U^{3+}) complexes, the selective complexation of U^{III} relatively to Ce^{III} by the Me_2pz ligand is predicted correctly, considering their total TBE_{frag} by both ZORA/BP86 (−1.287 vs −0.750 eV) and B3LYP (−1.042 vs −0.840 eV) computations. In fact, although the destabilizing steric effect (E_{ST}) is more important in uranium complexes relative to their cerium analogues, due to the shorter uranium−azine bond distances, it is significantly surpassed by the stabilizing effect of the orbital term E_{orb} contribution which appears to be a determining factor in this case. This issue has been largely discussed by Adamo and co-workers.[13a−c] For these systems, the bonding energy stabilization follows the electronic donation and back-donation effects within metal−ligand bonding.

As stated by previous works,[13a−c] it is worth noting that the high metallic charge induces a significant polarization of the ligands that contributes to the computed E_{orb} orbital energies. As M−N distances are similar for the U, Am, and Cm complexes, the polarization effects involved in E_{orb} are roughly the same and that the evolution of their orbital energies consequently follows that of orbital overlap. In the cases of their lanthanide counterparts (Ce, Nd, and Eu), M−N distances are longer, and the polarization effect should then be lower. In this manner, the Am^{III} E_{orb} is computed to be higher (in absolute value) that for its Eu^{III} congener (−1.34 vs −1.00 eV using BP86, and −2.202 vs. −1.525 eV with B3LYP). Thus, the Am species is found to be more stable due to a better orbital mixing and, in particular, strong ligand-to-metal donation effects as sustained by NPA electronic analysis (Table 5).

M−(C5-BPP) Energy Bonding. To validate our assumption of the reliability of the TBE_{frag} and/or E_{orb} as a criterion to compare the stability of the complexes, we consider now the $M(NO_3)_3$(C5-BPP) (M^{3+} = Ce, Nd, U, Eu, Am, Cm) species; the computed values are reported in Table 9.

According to our calculations, the computed U^{III} complexes systematically exhibit higher (in absolute value) total bonding energies (TBE_{frag}) than their Ce^{III} analogues, with a significantly higher orbital term E_{orb} in correlation with its more pronounced covalent character. Other differences with Ln^{III} systems are mainly due to the stronger steric terms in U^{III} complex which originate from shorter metal−ligand bond distances.

More notably, for the actual Eu^{III}/Am^{III} pair system, Am−L is computationally predicted to be slightly more stable than its Eu^{III} congener as the TBE_{frag} is computed slightly higher using BP86 (−3.70 vs −3.64 eV), and confirmed by B3LYP computations (−4.86 vs −4.28 eV) in agreement with the experimental findings.[15d] The stronger selectivity of the *N*-donor C5-BPP complexing ligand toward Am^{III} over Eu^{III} is well reproduced.[15d]

Figure 7a compares the total TBE of the different species (Table 9). As expected the TBEs in the case of the polyazine ligand are much higher than for the monoazine one, in relation with the higher number of metal−nitrogen bonds in the former ligand. This is in line with the higher selectivity for Ln^{III}/An^{III} differentiation which is observed for polyazine ligands.

dx.doi.org/10.1021/ic500361b | Inorg. Chem. 2014, 53, 4687−4697

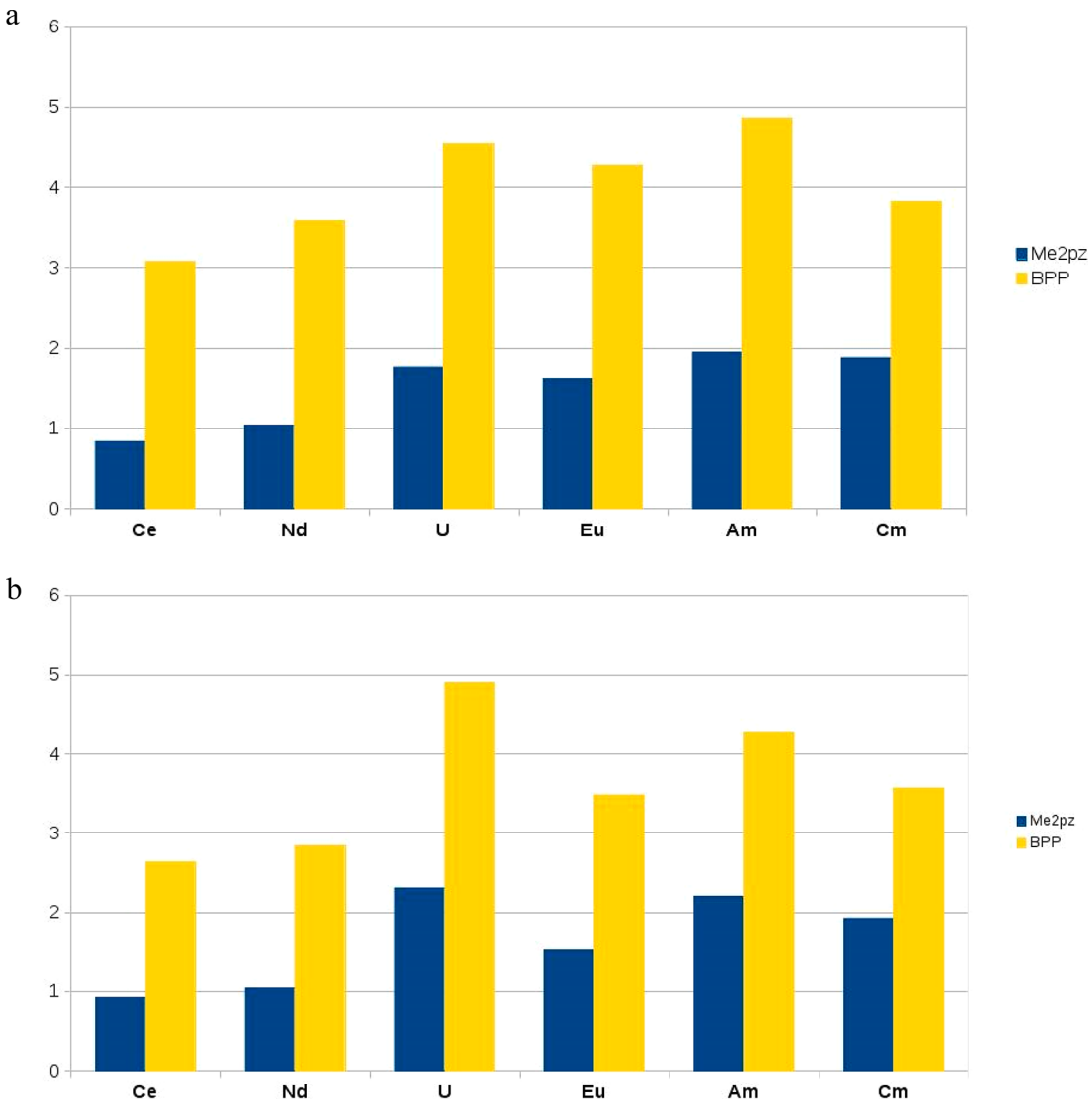

Figure 7. Total binding energy TBE_{frag} (eV) variation of the $M(TMSCp)_3(Me_2pz)$ and $M(NO_3)_3(C5\text{-}BPP)$ (M^{3+} = Ce, Nd, U, Eu, Am, and Cm) complexes computed at the ZORA/B3LYP level. (b) Orbital energy E_{orb} (eV) variation of the $M(TMSCp)_3(Me_2pz)$ and $M(NO_3)_3(C5\text{-}BPP)$ (M^{3+} = Ce, Nd, U, Eu, Am, and Cm) complexes computed at the ZORA/B3LYP level.

The results of Table 9 also reveal the significant role of the orbital term in stabilizing the An^{III} complex compared to Ln^{III} one. The E_{orb} strengthening for the Am species compared to the Eu(III) one (−4.27 vs. −3.48 eV B3LYP) confirms the previous assumption of stronger orbital mixing effects in the Am system, in agreement with a previous computational study,[13a] revealing a more covalent Cm system compared to the Gd one.

Thus, we find it interesting to compare the variation of this orbital term between the two classes of systems $M(TMSCp)_3(Me_2pz)$ and $M(NO_3)_3(C5\text{-}BPP)$. These trends are depicted in Figure 7b. As shown in this figure, this orbital term either for C5-BPP and Me_2pz ligands reaches its maximum for U^{III} systems. It is noteworthy that, for all complexes, the orbital term for polyazine BPP ligand is roughly twice its value for the monoazine Me_2pz, indicating that it increases with the number of M−N bonds. It is also likely to indicate a higher selectivity of the polyazine ligands toward Ln^{III}/An^{III} differentiation.

Interestingly, the comparison between Eu^{III} and Am^{III} shows a significantly greater orbital term for the latter which correlates well with the observed higher thermodynamic stability of minor actinides (Am^{III}, Cm^{III}) compared to Ln^{III}. This orbital term could also be a useful parameter to estimate the selectivity of different polyazine ligands. We plan to check this criterion considering other ligands of this kind.

CONCLUSIONS

Lanthanide and actinide MX_3L complexes (M^{+3} = Ce, Nd, Eu, U, Am; X = RCp^- and NO_3^-; L = N-donor ligand) related to Ln^{III}/An^{III} differentiation have been studied using scalar relativistic DFT computations. In the case of the Me_2pz monoazine ligand, our results bring to light the subtle balance between steric and covalent effects, combined with RCp/Me_2pz electron donor and acceptor abilities that, despite the important ionic character of M−L bonding, play a significant role in the Ln^{III}/An^{III} differentiation. We found also that Mayer, NPA, or Nalewajski−Mrozek bond indices correlate fairly well with the stretching frequencies of the M−N bonds which are indicators

dx.doi.org/10.1021/ic500361b | Inorg. Chem. 2014, 53, 4687−4697

of bond strengths. In the same way, complexes involving the polyazine ligand BPPR (R = H and neopentyl group C5) were studied; the comparison between C5BPP and BPPH reveals that the C5 substituting group reinforces the M−BPP bonding in agreement with experimental trends. Consideration of the total bonding energy TBE_{frag}, between the metallic fragment and the azine ligand, computed at the unrestricted DFT level, using either the BP86 or the B3LYP functional, permits us to reproduce correctly the relative stability of Eu^{III}/Am^{III} complexes and the observed greater affinity of BPP for minor An^{III} over Eu^{III} ions. Moreover, the orbital part E_{orb} of TBE_{frag} also correlates well with the relative selectivity of azine ligands toward Ln^{III}/An^{III} separation, and with the better selectivity of the polyazine relative to the monoazine ligand. These results show a way for future predictive design of highly selective ligands.

■ ASSOCIATED CONTENT

Supporting Information

Optimized coordinates, MO diagrams. This material is available free of charge via the Internet at http://pubs.acs.org.

■ AUTHOR INFORMATION

Corresponding Authors

*E-mail: lotfi.belkhiri@umc.edu.dz.

*E-mail: abdou.boucekkine@univ-rennes1.fr.

Notes

The authors declare no competing financial interest.

■ ACKNOWLEDGMENTS

We thank the French and Algerian governments for a research grant DPGRF/CNRS Project (2012-2014). The National Algerian Scientific Research Administration, NASR-ATRST (PNR Grant 8/u250/4169), is gratefully acknowledged for financial support. The authors are grateful to GENCI-IDRIS and GENCI-CINES for an allocation of computing time (Grant 2012-080649). The COST CM-1006 action is also acknowledged.

■ REFERENCES

(1) (a) Nash, K. L. In *Handbook on the Chemistry and Physics of Rare Earths*; Gschneidner, K. A., Jr., Eyring, L., Choppin, G. R., Lander, G. H., Eds.; Elsevier Science: Amsterdam, The Netherlands, 1994; Vol. *18*, Chapter 121. (b) *The Chemistry of the Actinide and Transactinide Elements*, 3rd ed.; Morss, L. R., Edelstein, N. M., Fuger, F., Eds.; Springer: Dordrecht, The Netherlands, 2006.

(2) Ephritikhine, M. *Dalton Trans.* **2006**, 2501.

(3) (a) Berthet, J. C.; Nierlich, M.; Ephritikhine, M. *Polyhedron* **2003**, *22*, 3475. (b) Mehdoui, T.; Berthet, J. C.; Thuéry, P.; Ephritikhine, M. *Eur. J. Inorg. Chem.* **2004**, 1996. (c) Weighl, M.; Denecke, M.; Panak, P. J.; Geist, A.; Gompper, K. *Dalton Trans.* **2005**, 1281. (d) Roger, M.; Barros, N.; Arliguie, T.; Thuéry, P.; Maron, L.; Ephritikhine, M. *J. Am. Chem. Soc.* **2006**, *128*, 8790. (e) Miguirditchian, M.; Guillaneux, D.; François, N.; Airvault, S.; Ducros, S.; Thauvin, D. *Nucl. Sci. Eng.* **2006**, *153*, 223.

(4) Rizkalla, E. N.; Choppin, G. R. In *Handbook on the Physics and Chemistry of Rare Earths*; Gschneidner, K. A., Eyring, L., Jr., Choppin, G. R., Lander, G. H., Eds. Elsevier Science: New York, 1994; Vol. *18*, p 529.

(5) Pearson, R. G. *Chemical Hardness*; Wiley-VCH: New York, 1997.

(6) Kolarik, Z. *Chem. Rev.* **2008**, *108*, 4208.

(7) Mehdoui, T.; Berthet, J. C.; Thuéry, P.; Ephritikhine, M. *Chem. Commun.* **2005**, 2860.

(8) Berthet, J. C.; Nierlich, M.; Miquel, Y.; Madic, C.; Ephritikhine, M. *Dalton Trans.* **2005**, 369.

(9) Mehdoui, T.; Berthet, J. C.; Thuéry, P.; Ephritikhine, M. *Dalton Trans.* **2005**, 1263.

(10) Mehdoui, T.; Berthet, J. C.; Thuéry, P.; Salmon, L.; Rivière, E.; Ephritikhine, M. *Chem.—Eur. J.* **2005**, *11*, 6994.

(11) (a) Miguirditchian, M.; Guillaneux, D.; Guillaumont, D.; Moisy, P.; Madic, C.; Jensen, M. P.; Nash, K. L. *Inorg. Chem.* **2005**, *44*, 1404. (b) Vetere, V.; Maldivi, P.; Adamo, C. *J. Comput. Chem.* **2003**, *24*, 850.

(12) (a) Kolarik, Z.; Müllich, U.; Gassner, F. *Ion Exch. Solvent Extr.* **1999**, *17*, 23. (b) Kolarik, Z.; Müllich, U.; Gassner, F. *Ion Exch. Solvent Extr.* **1999**, *17*, 1155. (c) Hudson, M. J.; Drew, M. G. B.; Foreman, M. S. St. J.; Hill, C.; Huet, N.; Madic, C.; Youngs, T. G. A. *Dalton Trans.* **2003**, 1675. (d) Berthet, J. C.; Rivière, C.; Miquel, Y.; Nierlich, M.; Madic, C.; Ephritikhine, M. *Eur. J. Inorg. Chem.* **2002**, 1439. (e) Berthet, J.-C.; Miquel, Y.; Iveson, P. B.; Nierlich, M.; Thuéry, P.; Madic, C.; Ephritikhine, M. *J. Chem. Soc., Dalton Trans.* **2002**, 3265. (f) Mazzanti, M.; Wietzke, R.; Pécaut, J.; Latour, J.-M.; Maldivi, P.; Remy, M. *Inorg. Chem.* **2002**, *41*, 2389. (g) Chan, G. Y. S.; Drew, M. G. B.; Hudson, M. J.; Isaacs, N. S.; Byers, P. *Polyhedron* **1996**, *15*, 3385. (h) Cordier, P. Y.; Hill, C.; Baron, P.; Madic, C.; Hudson, M. J.; Liljenzin, J. O. *J. Alloys Compd.* **1998**, *271*, 738.

(13) (a) Petit, L.; Adamo, C.; Maldivi, P. *Inorg. Chem.* **2006**, *45*, 8517. (b) Maldivi, P.; Petit, L.; Adamo, C.; Vetere, V. C. R. *Chimie* **2007**, *10*, 888. (c) Petit, L.; Daul, C.; Adamo, C.; Maldivi, P. *New J. Chem.* **2007**, *31*, 1738. (d) Petit, L. D. Sc. Thesis, Grenoble, 2007.

(14) Mehdoui, T.; Berthet, J. C.; Thuéry, P.; Ephritikhine, M. *Dalton Trans.* **2004**, 579.

(15) (a) Dam, H. H.; Reinhoudt, D. N.; Verboom, W. *Chem. Soc. Rev.* **2007**, *36*, 367. (b) Denecke, M. A.; Rossberg, A.; Panak, P. J.; Weigl, M.; Schimmelpfennig, B.; Geist, A. *Inorg. Chem.* **2005**, *44*, 8418. (c) Lewis, F. W.; Harwood, L. M.; Hudson, M. J.; Drew, M. G. B.; Modolo, G.; Sypula, M.; Desreux, J. F.; Bouslimani, N.; Vidick, G. *Dalton Trans.* **2010**, *39*, 5172. (d) Bremer, A.; Ruff, C. M.; Girnt, D.; Müllich, U.; Rothe, J.; Roesky, P. W.; Panak, P. J.; Karpov, A.; Müller, T. J. J.; Denecke, M. A.; Geist, A. *Inorg. Chem.* **2012**, *51*, 5199. (e) Steppert, M.; Císařová, I.; Fanghäne, T.; Geist, A.; Lindqvist-Reis, P.; Panak, P. J.; Štěpnička, P.; Trumm, S.; Walther, C. *Inorg. Chem.* **2012**, *51*, 591. (f) Trumm, S.; Lieser, G.; Foreman, M. R. S. J.; Panak, P. J.; Geist, A.; Fanghänel, T. *Dalton Trans.* **2010**, *39*, 923. (g) Lewis, F. W.; Harwood, L. M.; Hudson, M. J.; Drew, M. G. B.; Desreux, J. F.; Vidick, G.; Bouslimani, N.; Modolo, G.; Wilden, A.; Sypula, M.; Vuand, T.-H.; Simonin, J.-P. *J. Am. Chem. Soc.* **2011**, *133*, 13093.

(16) (a) Lan, J.-H.; Shi, W.-Q.; Yuan, L.-Y.; Zhao, Y.-L.; Li, J.; Chai, Z.-F. *Inorg. Chem.* **2011**, *50*, 9230. (b) Lan, J.-H.; Shi, W.-Q.; Yuan, L.-Y.; Li, J.; Zhao, Y.-L.; Chai, Z.-F. *Coord. Chem. Rev.* **2012**, *256*, 1406. (c) Lan, J.-H.; Shi, W.-Q.; Yuan, L.-Y.; Feng, Y.-X.; Zhao, Y.-L.; Chai, Z.-F. *J. Phys. Chem. A* **2012**, *116*, 504. (d) Lewis, F. W.; Harwood, L. M.; Hudson, M. J.; Drew, M. G. B.; Hubscher-Bruder, V.; Videva, V.; Arnaud-Neu, F.; Stamberg, K.; Vyas, S. *Inorg. Chem.* **2013**, *52*, 4993. (e) Benay, G.; Schurhammer, R.; Wipff, G. *Phys. Chem. Chem. Phys.* **2010**, *12*, 11089. (f) Benay, G.; Schurhammer, R.; Wipff, G. *Phys. Chem. Chem. Phys.* **2011**, *13*, 2922.

(17) (a) Keith, J. M.; Batista, E. R. *Inorg. Chem.* **2012**, *51*, 13. (b) Minasian, S. G.; Krinsky, J. L.; Arnold, J. *Chem.—Eur. J.* **2011**, *17*, 12234. (c) Hubscher-Bruder, V.; Haddaoui, J.; Bouhroum, S.; Arnaud-Neu, F. *Inorg. Chem.* **2010**, *49*, 1363. (d) Hudson, M. J.; Harwood, L. M.; Laventine, D. M.; Lewis, F. W. *Inorg. Chem.* **2013**, *52*, 3414. (e) Panak, P. J.; Geist, A. *Chem. Rev.* **2013**, *113*, 1199. (f) Gorden, A. E. V.; DeVore, M. A.; Maynard, B. A. *Inorg. Chem.* **2013**, *52*, 3445. (g) Whittaker, D. M.; Griffiths, T. L.; Helliwell, M.; Swinburne, A. N.; Natrajan, L. S.; Lewis, F. W.; Harwood, L. M.; Parry, S. A.; Sharrad, C. A. *Inorg. Chem.* **2013**, *52*, 3429. (h) de Sahb, C.; Watson, L. A.; Nadas, J.; Hay, B. P. *Inorg. Chem.* **2013**, *52*, 10632.

(18) te Velde, G.; Bickelhaupt, F. M.; van Gisbergen, S. J. A.; Fonseca Guerra, C.; Baerends, E. J.; Snijders, J. G.; Ziegler, T. *J. Comput. Chem.* **2001**, *22*, 931 and references therein.

(19) Fonseca Guerra, C.; Snijders, J. G.; te Velde, G.; Baerends, E. J. *Theor. Chem. Acc.* **1998**, *99*, 391.

(20) *ADF2012.01*; SCM, Theoretical Chemistry, Vrije Universiteit: Amsterdam, The Netherlands, http://www.scm.com.
(21) (a) Vosko, S. D.; Wilk, L.; Nusair, M. *Can. J. Chem.* **1990**, *58*, 1200. (b) Becke, A. D. *Phys. Rev. A* **1988**, *38*, 3098. (c) Perdew, J. P. *Phys. Rev. B* **1986**, *34*, 7406. (d) Becke, A. D. *J. Chem. Phys.* **1993**, *98*, 5648. (e) Lee, C.; Yang, W.; Parr, R. G. *Phys. Rev. B* **1988**, *37*, 785.
(22) (a) Roger, M.; Belkhiri, L.; Thuéry, P.; Arliguie, T.; Fourmigué, M.; Boucekkine, A.; Ephritikhine, M. *Organometallics* **2005**, *24*, 4940. (b) Roger, M.; Belkhiri, L.; Arliguie, T.; Thuéry, P.; Boucekkine, A.; Ephritikhine, M. *Organometallics* **2008**, *27*, 33. (c) Roger, M.; Belkhiri, L.; Thuéry, P.; Bouaoud, S. E.; Boucekkine, A.; Ephritikhine, M. *Inorg. Chem.* **2009**, *48*, 221. (d) Meskaldji, S.; Belkhiri, L.; Arliguie, T.; Fourmigué, M.; Ephritikhine, M.; Boucekkine, A. *Inorg. Chem.* **2010**, *49*, 3192.
(23) (a) Shamov, G. A.; Schreckenbach, G. *J. Phys. Chem. A* **2005**, *109*, 10961. (b) Schelter, E. J.; Yang, P.; Scott, B. L.; Thompson, J. D.; Martin, R. L.; Hay, P. J.; Morris, D. E.; Kiplinger, J. L. *Inorg. Chem.* **2007**, *46*, 7477. (c) Gaunt, A. J.; Reilly, S. D.; Enriquez, A. E.; Scott, B. L.; Ibers, J. A.; Sekar, P.; Ingram, K. I. M.; Kaltsoyannis, N.; Neu, M. P. *Inorg. Chem.* **2008**, *47*, 29. (d) Graves, C. R.; Yang, P.; Kozimor, S. A.; Vaughn, A. E.; Clark, D. L.; Conradson, E. S. D.; Schelter, E. J.; Scott, B. L.; Thompson, J. D.; Hay, P. J.; Morris, D. E.; Kiplinger, J. L. *J. Am. Chem. Soc.* **2008**, *130*, 5272. (e) Gaunt, A. J.; Reilly, S. D.; Enriquez, A. E.; Scott, B. J.; Ibers, J. A.; Sekar, P.; Ingram, K. I. M.; Kaltsoyannis, N.; Neu, M. P. *Inorg. Chem.* **2008**, *47*, 29.
(24) (a) Reed, A. E.; Weinstock, R. B.; Weinhold, F. *J. Chem. Phys.* **1985**, *83*, 735. (b) Foster, J. P.; Weinhold, F. *J. Am. Chem. Soc.* **1980**, *102*, 7211. (c) Reed, A. E.; Curtiss, L. A.; Weinhold, F. *Chem. Rev.* **1988**, *88*, 899. (d) Bader, R. F. W. *Atoms in Molecules: A Quantum Theory*; OUP: Oxford, 1990. (e) Mulliken, R. S. *J. Chem. Phys.* **1955**, *23*, 1833. (f) Petit, L.; Joubert, L.; Maldivi, P.; Adamo, C. *J. Am. Chem. Soc.* **2006**, *128*, 2190.
(25) (a) Mountain, A. R. E.; Kaltsoyannis, N. *Dalton Trans.* **2013**, *42*, 13477. (b) Jones, M. B.; Gaunt, A. J.; Gordon, J. C.; Kaltsoyannis, N.; Neu, M. P.; Scott, B. L. *Chem. Sci.* **2013**, *4*, 1189. (c) Schnaars, D. D.; Gaunt, A. J.; Hayton, T. W.; Jones, M. B.; Kirker, I.; Kaltsoyannis, N.; May, I.; Reilly, S. D.; Scott, B. L.; Wu, G. *Inorg. Chem.* **2012**, *51*, 8557. (d) Arnold, P. L.; Turner, Z. R.; Kaltsoyannis, N.; Pelekanaki, P.; Bellabarba, R. M.; Tooze, R. P. *Chem.—Eur. J.* **2010**, *16*, 9623. (e) Vlaisavljevich, B.; Miró, P.; Cramer, C. J.; Gagliardi, L.; Infante, I.; Liddle, S. T. *Chem.—Eur. J.* **2011**, *17*, 8424.
(26) (a) Morokuma, K. *J. Chem. Phys.* **1971**, *55*, 1236. (b) Kitaura, K.; Morokuma, K. *Int. J. Quantum Chem.* **1976**, *10*, 325. (c) Ziegler, T.; Rauk, A. *Theor. Chim. Acta* **1977**, *46*, 1. (d) Mayer, I. *Chem. Phys. Lett.* **1983**, *7*, 270. (e) Haller, L. J. L.; Kaltsoyannis, N.; Sarsfield, M. J.; May, I.; Cornet, S. M.; Redmond, M. P.; Helliwell, M. *Inorg. Chem.* **2007**, *46*, 4868. (f) Nalewajski, R. F.; Mrozek, J. *Int. J. Quantum Chem.* **1994**, *51*, 187. (g) Nalewajski, R. F.; Mrozek, J.; Michalak, A. *Int. J. Quantum Chem.* **1997**, *6*, 589. (h) Michalak, A.; De Kock, R. L.; Ziegler, T. *J. Phys. Chem. A* **2008**, *112*, 7256. (i) Curley, J. J.; Piro, N. A.; Cummins, C. C. *Inorg. Chem.* **2009**, *48*, 9599. (j) Patel, D.; Moro, F.; McMaster, J.; Lewis, W.; Blake, A. J.; Liddle, S. T. *Angew. Chem.* **2011**, *123*, 10572. (k) David, P.; Mills, D. P.; Moro, F.; McMaster, J.; van Slageren, J.; Lewis, W.; Blake, A. J.; Liddle, S. T. *Nat. Chem.* **2011**, *3*, 454. (l) Fox, A. R.; Cummins, C. C. *J. Am. Chem. Soc.* **2009**, *131*, 5716.
(27) (a) Kaltsoyannis, N. *Inorg. Chem.* **2013**, *52*, 3407. (b) Neidig, M. L.; Clark, D. L.; Martin, R. L. *Coord. Chem. Rev.* **2013**, *257*, 394.
(28) Shannon, R. D. *Acta Crystallogr., Sect. A* **1976**, *32*, 751.

dx.doi.org/10.1021/ic500361b | *Inorg. Chem.* 2014, 53, 4687−4697